

Accepted Manuscript



Rapid and scalable synthesis of chiral porphyrin cage compounds

Pieter J. Gilissen, Anne Swartjes, Bram Spierenburg, Jeroen P.J. Bruekers, Paul Tinnemans, Paul B. White, Floris P.J.T. Rutjes, Roeland J.M. Nolte, Johannes A.A.W. Elemans

PII: S0040-4020(19)30751-3

DOI: <https://doi.org/10.1016/j.tet.2019.07.009>

Reference: TET 30451

To appear in: *Tetrahedron*

Received Date: 18 May 2019

Revised Date: 1 July 2019

Accepted Date: 5 July 2019

Please cite this article as: Gilissen PJ, Swartjes A, Spierenburg B, Bruekers JPJ, Tinnemans P, White PB, Rutjes FPJT, Nolte RJM, Elemans JAAW, Rapid and scalable synthesis of chiral porphyrin cage compounds, *Tetrahedron* (2019), doi: <https://doi.org/10.1016/j.tet.2019.07.009>.

This is a PDF file of an unedited manuscript that has been accepted for publication. As a service to our customers we are providing this early version of the manuscript. The manuscript will undergo copyediting, typesetting, and review of the resulting proof before it is published in its final form. Please note that during the production process errors may be discovered which could affect the content, and all legal disclaimers that apply to the journal pertain.

Graphical Abstract

To create your abstract, type over the instructions in the template box below.
 Fonts or abstract di

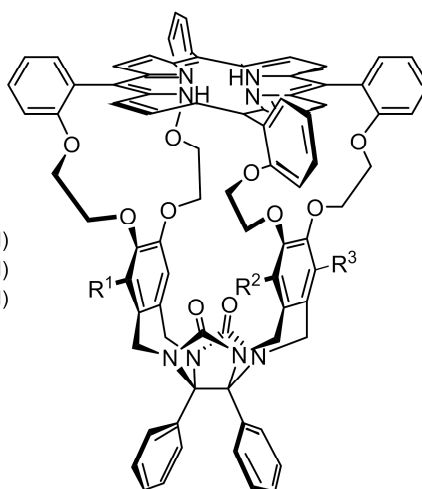
Rapid and scalable synthesis of chiral porphyrin cage compounds

Leave this area blank for abstract info.

Pieter J. Gilissen, Anne Swartjes, Bram Spierenburg, Jeroen P. J. Bruekers, Paul Tinnemans, Paul B. White, Floris P.J.T. Rutjes, Roeland J.M. Nolte, Johannes A.A.W. Elemans

Radboud University, Institute for Molecules and Materials, Heyendaalseweg 135, 6525 AJ, Nijmegen, The Netherlands. E-mail J.Elemans@science.ru.nl, R.Nolte@science.ru.nl

H_21 ($R^1 = R^2 = R^3 = H$)
 H_22 ($R^1 = NO_2, R^2 = R^3 = H$)
 H_23 ($R^1 = R^3 = NO_2, R^2 = H$)
 H_24 ($R^1 = R^2 = NO_2, R^3 = H$)



An improved and scalable synthetic route to molecular catalytic machines, to encode information onto polymers, has been developed. Regioselective nitration reactions have been performed to introduce chirality on the catalyst. The mechanism behind the regioselectivity is herein investigated.

Rapid and scalable synthesis of chiral porphyrin cage compounds

Pieter J. Gilissen[#], Anne Swartjes[#], Bram Spierenburg, Jeroen P.J. Bruekers, Paul Tinnemans, Paul B. White, Floris P.J.T. Rutjes, Roeland J.M. Nolte*, Johannes A.A.W. Elemans*

Radboud University, Institute for Molecules and Materials, Heyendaalseweg 135, 6525 AJ, Nijmegen, The Netherlands. E-mail J.Elemans@science.ru.nl, R.Nolte@science.ru.nl

[#]These authors contributed equally to this research

Abstract

An improved and scalable synthetic route to chiral porphyrin cage compounds, which will be used as catalytic machines for the encoding of information into polymers, has been developed. The porphyrin cage was made chiral by introducing one or two nitro groups on its xylylene sidewalls. This nitration was performed with fuming nitric acid at low temperature and occurred in a highly regioselective fashion. The latter was thought to be the result of the binding of a nitronium cation inside the cavity of the cage compound, directing the reaction to the sidewalls. However, ¹H NMR titrations of the porphyrin cage compound with either nitric acid or the nitronium salt [NO₂][BF₄] revealed that the effect of the host-guest binding of the nitronium ion on the selectivity of the reaction is negligible. Instead, protonation of the porphyrin plays an essential role as it prevents the ring from being oxidized, allowing the nitration to be directed to the sidewalls.

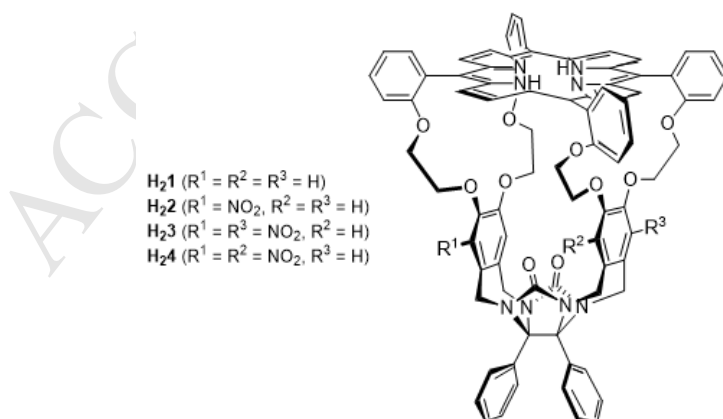
Keywords: Glycoluril; Porphyrin; Host-guest chemistry; Cage molecule; Chirality; Nitration.

1. Introduction

The amount of information that is produced nowadays is increasing exponentially and will lead to storage problems in the near future^{1,2}. As a result, new approaches to store data are currently being developed and an interesting option is to use biological (e.g. DNA) and synthetic polymers for this purpose³⁻⁷. We have started a program to write and store digital information onto polymers in the form of chemical functions with the help of catalytic machines that thread onto a polymer chain, and while moving along it, write (*R,R*)- and (*S,S*) epoxides representing the digits 0 and 1^{8,9}. The aforementioned catalytic machines are based

on a chiral manganese(III) porphyrin cage compound derived from diphenylglycoluril. The synthesis of the parent achiral porphyrin cage compound **H₂1** (Figure 1) was first reported in 1999, and required 9 steps¹⁰. Later in 2007 the first improvements on the laborious synthesis of the porphyrin cage were made¹¹. With the challenging goals of writing and storing information on polymers with catalytic machines in mind, our aim is to further reduce the number of synthetic steps and to increase the overall yield, such that also substantial amounts of chiral derivatives of **H₂1**, i.e. compounds **H₂2** and **H₂3**, are easily accessible. These compounds are the starting materials for the machines that can write chiral epoxides.

The introduction of chirality into the porphyrin cage compound (**H₂2** and **H₂3**) was reported in an earlier study¹², i.e. by treating cage compound **H₂1** with fuming nitric acid, which lead to functionalization of exclusively the xylylene sidewalls with one or two nitro-groups. In addition to conferring chirality, the nitro groups also serve as excellent handles to further functionalize the cage¹³. Remarkably, the nitration occurred in a highly regioselective fashion, which was initially thought to be a consequence of a nitronium cation being bound in the cavity of the cage compound¹². Because of its proximity it would then only nitrate the aromatic rings of the sidewalls. Interestingly, it has been reported that a simple nitration of *meso*-tetraphenylporphyrin (TPP) with HNO₃ can nitrate the β -pyrroles, as well as the phenyl rings¹⁴⁻¹⁷. Other work on the nitration of *meso*-aryl porphyrins using a radical¹⁸ (NO₂•) or anionic¹⁹ (NO₂⁻) nitro-source revealed selectivity of nitration for the β -pyrrolic positions of the porphyrin ring. These previous findings suggest that vastly different mechanisms are at play during the nitration of **H₂1**. In the present study, we address this issue further by performing additional studies that aim to shine light on the mechanism behind the observed

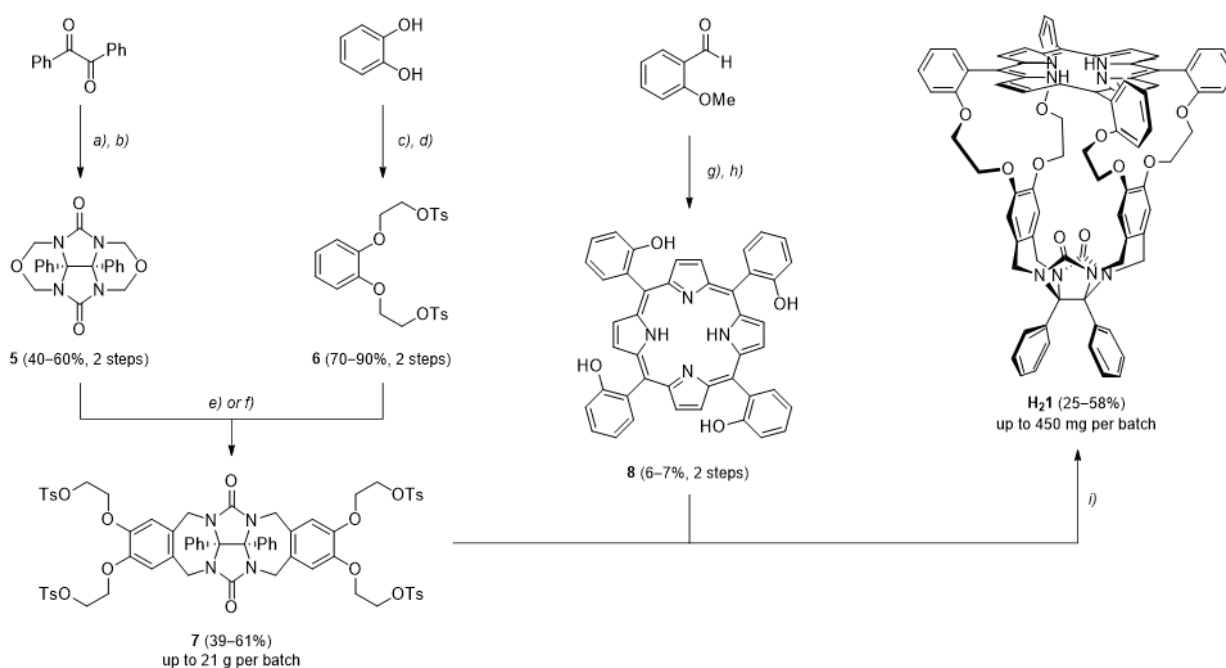


regioselectivity.

Figure 1. Porphyrin cage compounds

2. Results and discussion

Our improved and shorter synthetic route towards the parent porphyrin cage compound **H₂1** is shown in Scheme 1. The synthetic strategy encompasses two parts: the synthesis of the tetratosyl clip compound (**7**) and the synthesis of the porphyrin roof (**8**). The clip molecule was constructed starting from diphenylglycoluril, which was prepared in up to quantitative yield (70–99%) by the acid-catalyzed condensation of benzil and urea in toluene using a Dean–Stark apparatus. Because diphenylglycoluril is hardly soluble in any common organic solvent, it was further functionalized to cyclic ether **5** in reasonable yield (50–70%) by a reaction with formaldehyde and a subsequent acid-catalyzed ring closing reaction. Cyclic ether **5** is a weak electrophile in Friedel–Crafts alkylation reactions and, hence, in the past more reactive intermediates were synthesized from this compound for the attachment of the aromatic sidewalls (see Supporting Information, Scheme S1). These sidewalls are derived from pyrocatechol. Previously, the direct bis-alkylation of this compound with 2-chloroethanol turned out to be cumbersome, as the product was formed in low yield (<30%). We found that under the reaction conditions, 2-chloroethanol is transformed into oxirane (detected by ¹H NMR), which either reacts with deprotonated catechol, or leaves the reaction mixture as a gaseous byproduct. By keeping the pH of the reaction mixture between 9 and 11, catechol was always present in its deprotonated form. In this way, a multigram scale alkylation of catechol with 2-chloroethanol in water gave the diol intermediate in quantitative yield, without the need for further purification. Subsequent tosylation of the hydroxy groups afforded the sidewall molecule **6** in good yield after a single recrystallization step.



Scheme 1. Synthesis of cage compound **H₂1**. Reagents and conditions: *a*) CO(NH₂)₂, TFA, PhMe, reflux; *b*) HCHO, NaOH, DMSO/H₂O, 20 °C; then HCl, reflux; *c*) 2-chloroethanol, KOH, H₂O, 60 °C; *d*) TsCl, pyridine, DCM, 0 → 20 °C; *e*) SOCl₂, ZnCl₂, DCM, 20 °C; *f*) SOCl₂, Sn(OTf)₂ (cat.), DCM, 20 °C; *g*) pyrrole, EtCO₂H, reflux; then DDQ, CHCl₃, reflux; *h*) BBr₃, DCM, -25 → 20 °C; *i*) K₂CO₃, MeCN, reflux.

The Friedel–Crafts alkylation reaction between **6** and the tetrachloromethyl derivative (see Supporting Information, Scheme S1) of **5** had always been performed under reflux conditions in 1,2-dichloroethane, moderated by a stoichiometric amount of tin(IV) chloride as the Lewis acid, to furnish clip molecule **7** in moderate yield (typically 30–60%). It is assumed that the Lewis acid activates the carbon-chlorine bond to form an *N*-acyliminium intermediate, which is prone to nucleophilic attack from the electron-rich arene **6**. We reasoned that the same *N*-acyliminium intermediate will be present in any conversion of **5** to a more reactive *N,O*-acetal derivative. Hence, a one-pot activation and Friedel–Crafts alkylation reaction should work, starting from cyclic ether **5** or any similar *N,O*-acetal (Supporting Information, Table S1). We found that cyclic ether **5** could be activated in situ with thionyl chloride and a stoichiometric amount of a Lewis acid (e.g. zinc chloride) to furnish the clip molecule in reasonable yield after a single trituration of the crude product as the sole purification step. The reaction also worked with a catalytic amount of Lewis acid (e.g. tin(II) trifluoromethanesulfonate), again providing clip molecule **7** in reasonable yield. The same conditions were used in multigram scale experiments (up to 21 g) without significant yield losses. Now, tosyl clip **7** can be obtained in fewer steps and with an increased overall yield (31%) as compared to earlier work (11%)^{10,11}.

The porphyrin roof (**8**) was synthesized in two steps from 2-methoxybenzaldehyde and pyrrole in a reproducible yield of 6-7%, which could not be improved further. The methyl ether was chosen as a protecting group to simplify the workup during the porphyrin synthesis. The protecting group was easily removed in quantitative yield via a reaction with boron tribromide.

Finally, a highly diluted 1:1 mixture of tosyl clip **7** and porphyrin roof **8** was refluxed in acetonitrile, with potassium carbonate as a base, to yield free base porphyrin cage compound **H₂1** in acceptable yield (typically 25–58%) after purification by a single chromatographic event. The yield of the cage synthesis was highly dependent on the duration of the reaction. As described previously^{10,11}, a yield of 25–30% was obtained after just 1 day, while a yield of up to an impressive 58% can be reached reproducibly by refluxing the mixture for approximately 10 days, as we show here. As such, up to 450 mg of porphyrin cage compound

H₂1 could be obtained per batch. The physical properties of this compound were in line with our previous reports. An X-ray structure of **H₂1** could be determined after crystallization of this compound from CDCl₃ at -60 °C (Figure 2). This chloroform solvate is a pseudo-polymorph of an X-ray structure of the same cage compound, reported by us before, which was a chloroform-acetonitrile solvate²⁰. In the current structure, **H₂1** contains two chloroform molecules in the asymmetric unit, both disordered over two positions (Figure 2b). Interestingly, one of these solvent molecules is hosted by the cavity of **H₂1**.

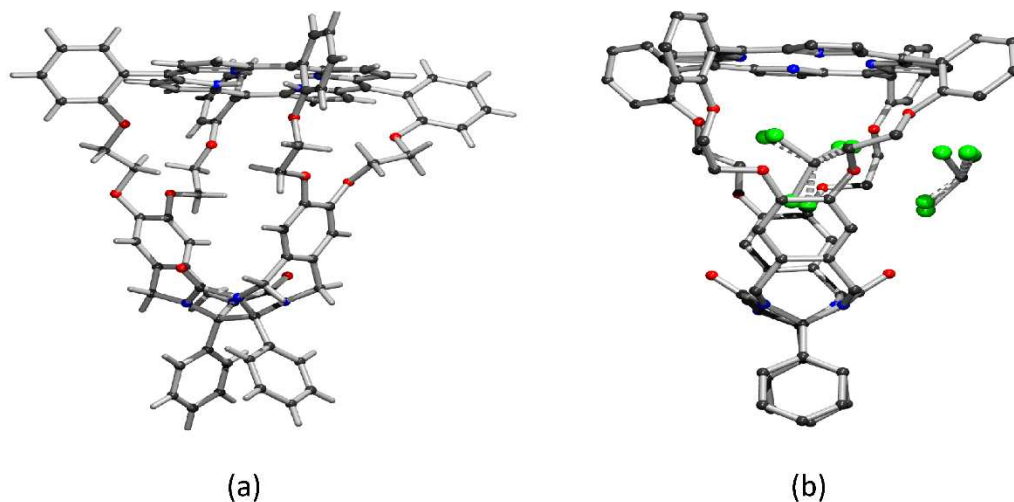
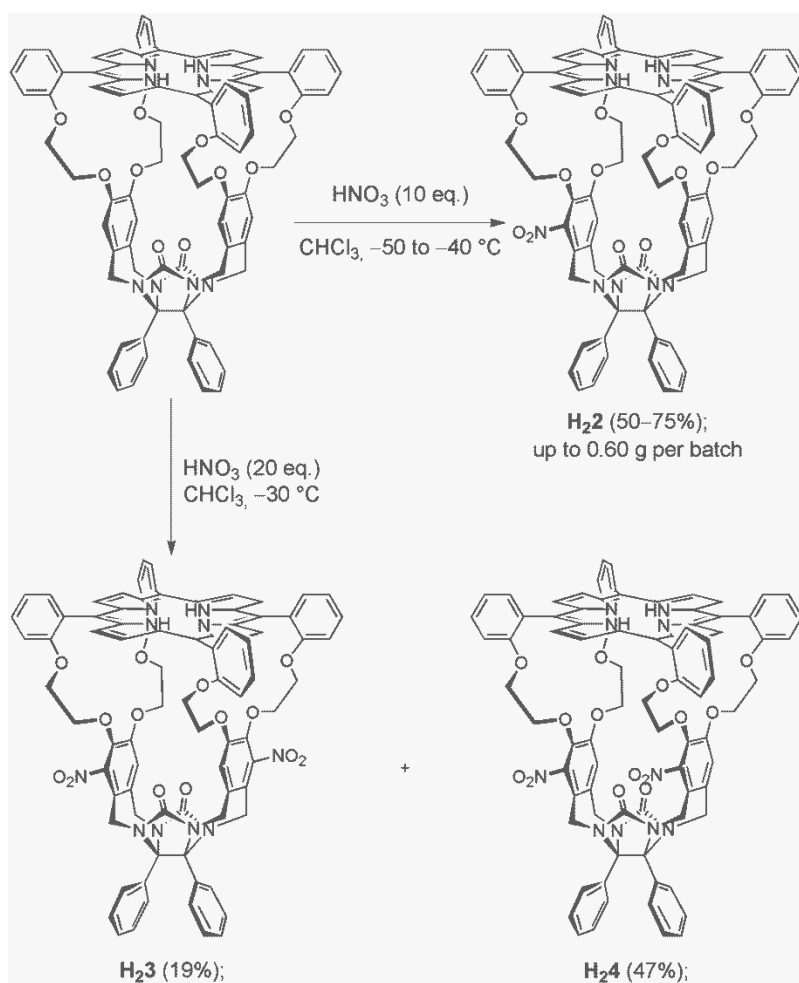


Figure 2. X-ray structure of compound **H₂1** (a) excluding and (b) including co-crystallized chloroform solvent molecules.

Functional handles can be added selectively to the xylylene side walls of **H₂1** in the form of either one nitro-group, creating the chiral mono-nitrated cage **H₂2**, or two nitro-groups, leading to the chiral *anti*-di-nitro cage **H₂3** and the achiral *syn*-di-nitro cage **H₂4** (Scheme 2). This is achieved by reacting the cage with fuming nitric acid at low temperature, as we reported earlier¹².



Scheme 2. Synthesis of cage compounds **H₂2**, **H₂3** and **H₂4**.

We noticed that the formation of either the mono- or the di-nitro products is very sensitive to changes in the concentration of the reactants and the temperature. When the temperature of the reaction mixture in chloroform is strictly kept between -50 and -40 °C, the major product is the mono-nitro-compound **H₂2**, which can be isolated in a yield of up to 75% (but typically 50–60%). The di-nitro products **H₂3** and **H₂4** already quickly form when the temperature is slightly increased. In an attempt to elucidate the kinetic factors of the nitration reaction, we monitored its progress over time with the help of ^1H NMR spectroscopy (Figure 3). We used a ten times more dilute concentration of **H₂1** (0.743 mM) than is normally used during the reaction, because in that case it is possible to perform the NMR experiments at a milder temperature (0 °C). This temperature grants us a longer timespan to perform the measurements before completion of the reaction, and although the yield of **H₂2** is somewhat lower, the reaction is easier to handle and to reproduce. Over time, we observed the consumption of **H₂1** and the formation of **H₂2** and **H₂4**; the formation of **H₂3** was very slow and was therefore not considered in the kinetics plot. All changes in concentration are fitted

using first order kinetics. Therefore, it appears that the formation of **H₂2** follows a first order kinetic process. However, the conversion rate could not be accurately determined since it became clear that the concentration of **H₂1** was decreasing with a much faster rate than **H₂2** and **H₂4** were formed. Hence, it became clear that the mass balance did not remain constant, indicating decomposition. The longer the reaction ran, the more decomposition occurred. TLC analysis also confirmed the formation of degradation products. It was unclear whether either the starting material or the nitrated products decomposed, or both of these. However, the apparent decomposition implied that a short reaction time would be optimal, which could indeed be achieved by using a higher concentration of **H₂1** in combination with lower temperatures.

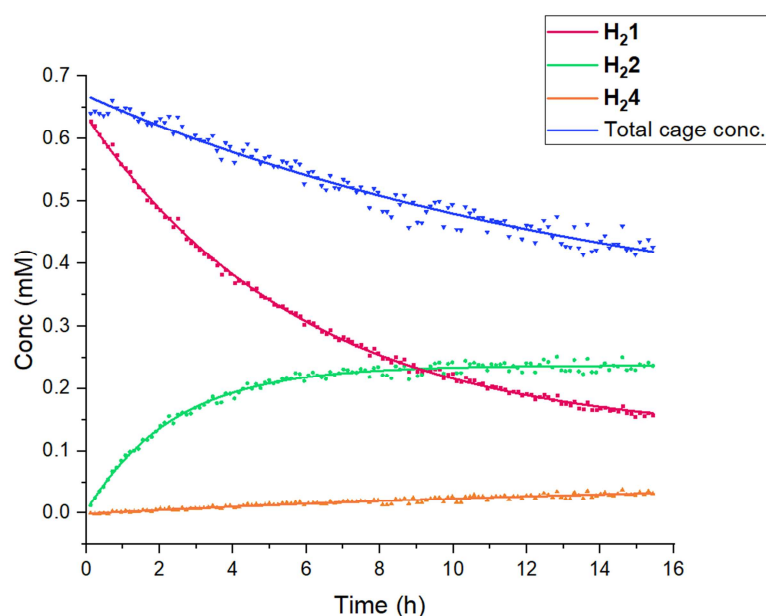


Figure 3. Progress of the nitration of **H₂1** (initial concentration 0.743 mM) as a function of time. T = 0 °C in CDCl₃, concentrations are based on integration of relevant signals in the ¹H NMR spectra. For the calculation of the concentrations, dibromomethane was used as internal standard.

Because of the observed sensitivity of the reaction to the nitration conditions, we attempted to introduce the nitro-groups in an earlier stage. When we treated clip molecule **7** with fuming nitric acid under the same conditions, the material decomposed and no nitrated product could be isolated or starting material recovered. This might indicate that the cage plays a role in facilitating the nitration reaction, as we reported previously¹². Another possibility was to nitrate compound **6**, but this reaction led to nitration at the meta-position of the

dialkoxybenzene ring, which would make it impossible to obtain the nitrated version of **7** in the subsequent step. Alternatively, **H₂1** was subjected to a mild nitration method with ammonium nitrate and trifluoroacetic acid anhydride in chloroform at room temperature, to investigate if a higher selectivity for the mono-nitrated product and a lower amount of decomposition could be achieved. Instead, the previously observed regioselectivity for the sidewalls, was lost, and an inseparable mixture of many different nitrated products was generated. The observation that the nitration occurred regioselectively with nitric acid and non-selectively with ammonium nitrate could indicate that the cationic nature of the nitronium ion plays an important role, since this cation is not formed under the mild nitration conditions of the latter reagent.

To further investigate whether the observed sidewall selectivity was caused by the inclusion of the nitronium cation in the cavity of the cage compound during the nitration reaction, several ¹H NMR titrations were performed. When a solution of cage molecule **H₂1** was titrated with HNO₃, the NMR signals corresponding to the β-pyrrole protons (protons **a** in Figure 4) and those belonging to the *meso*-phenyl rings (**b**) attached to the porphyrin roof showed broadening. This is indicative of proton-exchange after the porphyrin is mono-protonated. These signals became well-defined and sharp again after the addition of ~2 equivalents of fuming nitric acid, which suggests bis-protonation of the porphyrin roof (Figure 4). Furthermore, the pyrrole-NH signal (**g**, -2.70 ppm) was no longer observed after the addition of HNO₃, due to broadening of the signal as a result of exchange with water.

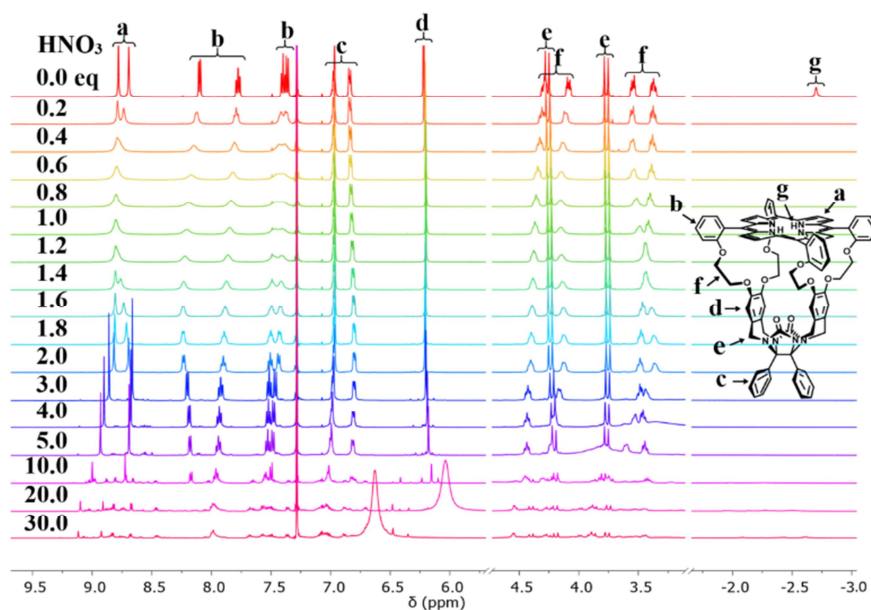


Figure 4. ^1H NMR titration of **H₂1** with HNO_3 . Each ^1H NMR spectrum was recorded after the addition of the indicated amount of HNO_3 . The signals are assigned to different parts of the cage compound, see structure on the right. Solvent CDCl_3 .

After the addition of 3.0 equivalents of HNO_3 , the formation of **H₂2** could be observed through the upcoming three singlets of the xylylene sidewall protons (**d**). This indicates that 2 equivalents of nitric acid are needed to protonate the porphyrin roof prior to nitration. When less than 2 equivalents of nitric acid were added, the ^{14}N NMR spectrum of the mixture only showed the signal of nitrate anions, which suggests that HNO_3 protonates the porphyrin roof, leaving NO_3^- behind. After the addition of 2 equivalents, the signal corresponding to nitric acid appeared in the ^{14}N NMR spectrum as well (Supporting Information, Figure S1). If a nitronium cation had been bound inside the cavity, ^{14}N NMR should have shown an additional signal belonging to the shielded cationic nitronium guest. As expected, ^{14}N signals that would arise from the porphyrin cages are not observed, since ^{14}N signals in larger molecules and in an asymmetric environment are broadened because of quadrupolar interactions. In another ^1H NMR titration, nitronium tetrafluoroborate was used as a potential nitronium source (Figure 5).

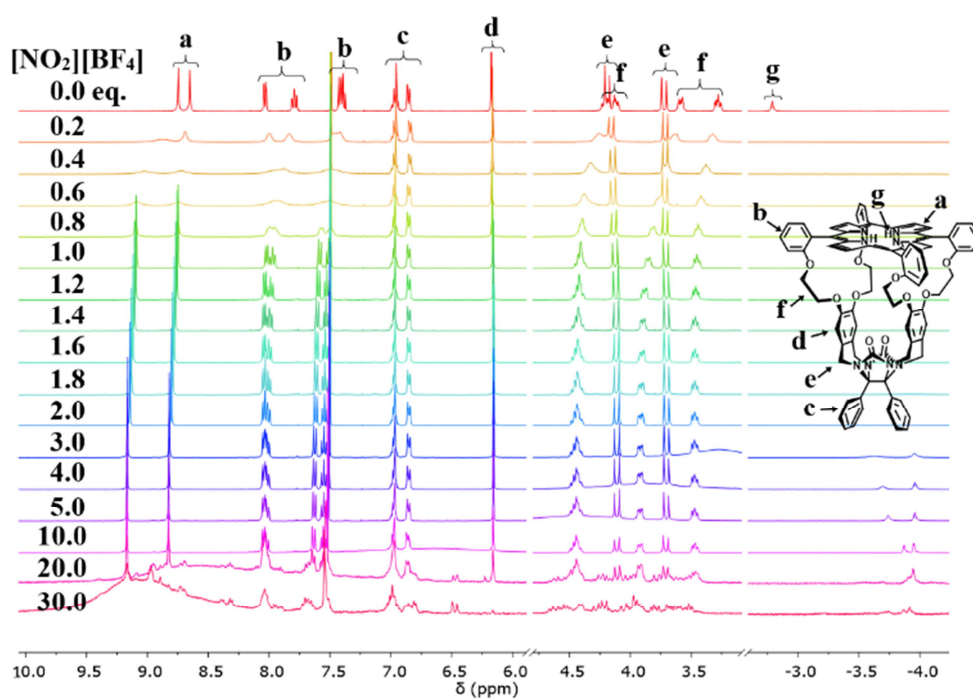


Figure 5. ^1H NMR titration of **H₂1** (in CDCl_3) with $[\text{NO}_2][\text{BF}_4]$ (in CD_3CN). Each ^1H NMR spectrum was recorded after the addition of the indicated amount of $[\text{NO}_2][\text{BF}_4]$. The signals are assigned to different parts of the cage compound, see structure on the right.

Similar to the titration with HNO_3 , broadening of the signals corresponding to the porphyrin roof (**a**, **b**, **g**) occurred after adding the salt. After the addition of ~ 1 equivalent of $[\text{NO}_2][\text{BF}_4]$, a well-defined spectrum was obtained again, indicating either bis-protonation of the porphyrin, or the presence of a 1:1 host-guest complex of the porphyrin cage with either a nitronium or a nitrate ion. After the addition of 10 equivalents of $[\text{NO}_2][\text{BF}_4]$, nitration of the sidewalls could be observed through the three growing singlets at between 6.50 and 6.25 ppm. These peaks continued to grow upon the addition of more of the nitronium salt. In the presence of less than 1 equivalent of the salt, the ^{14}N NMR spectrum again revealed the presence of nitrate as the only symmetric nitrogen-containing species. Upon the addition of more of the salt, the signal corresponding to nitric acid appeared in the ^{14}N NMR spectrum as well (Supporting Information, Figure S2). Combined with trace amounts of water, each nitronium tetrafluoroborate ion pair can act as a diprotic acid. To further support these findings, the ^1H NMR spectrum of **H₂1** in the presence of 1.0 equiv. of $[\text{NO}_2][\text{BF}_4]$ was compared to a spectrum of **H₂1** in the presence of TFA (5.0 equiv, to ensure bis-protonation of the porphyrin) (Figure 6). It is obvious that the two spectra are basically the same, apart

from small deviations that are probably caused by the different anions. Hence, it is very likely that protonation of the porphyrin is the initial event during the nitration reaction, which is in line with the observed color change from purple to green when the fuming HNO_3 is added to the solution of **H₂1**.

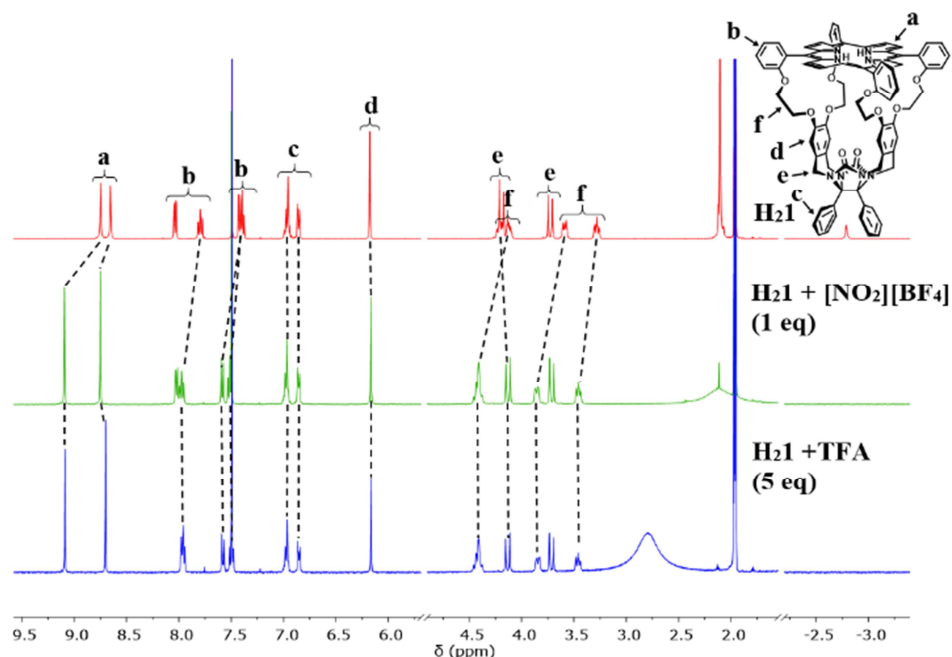


Figure 6. (Top) ^1H NMR spectrum of **H₂1**. (Middle) ^1H NMR spectrum of **H₂1** in the presence of 1 equivalent of $[\text{NO}_2][\text{BF}_4]$. (Bottom) ^1H NMR spectrum of **H₂1** in the presence of 5 equivalents of TFA. Solvent $\text{CDCl}_3\text{-CD}_3\text{CN}$ (1:1, v/v).

In a final attempt to probe the presence of a nitronium cation in the cavity of the cage molecule during the nitration reaction, a nickel(II) ion was inserted in the porphyrin ring to afford a stable 16 electron square planar diamagnetic complex **Ni1**, which also resists protonation of the porphyrin (Figure 7, top ^1H NMR spectrum). When a solution of **Ni1** in chloroform-acetonitrile (1:1, v/v) was treated with 1.0 equiv. of $[\text{NO}_2][\text{BF}_4]$, a new symmetric compound was formed (Figure 7, bottom ^1H NMR spectrum). Its ^1H NMR spectrum showed the absence (or extreme broadening) of all the β -pyrrole resonances of the porphyrin (**a**). Moreover, the signals of the *meso*-phenyl substituents (**b**) were significantly broadened as compared to those in the spectrum of **Ni1**. The signals arising from the diphenylglycoluril clip part (**c**, **e**) remained basically unaffected. We propose that in the case of **Ni1** the nitronium cation serves as a one-electron oxidant, which oxidizes the porphyrin to a radical cation which

is delocalized over the entire porphyrin ring system. Hence, the porphyrin resonances in the ^1H NMR spectrum become extremely broadened, and protons in the vicinity of the porphyrin experience a similar but smaller effect. These paramagnetic effects are highly dependent on the distance to the paramagnetic center, and as a result proton signals further away from it are less affected.

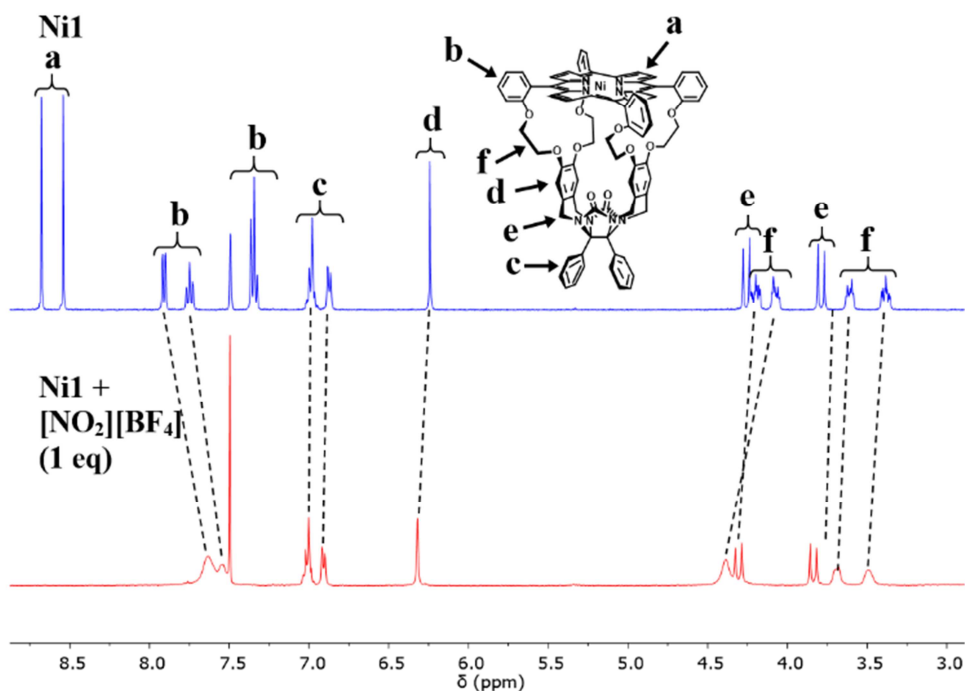


Figure 7. (Top) ^1H NMR spectrum of **Ni1**. (Bottom) ^1H NMR spectrum of **Ni1** in the presence of 1 equivalent of $[\text{NO}_2][\text{BF}_4]$. Solvent $\text{CDCl}_3\text{-CD}_3\text{CN}$ (1:1, v/v).

Alternative to the formation of a radical cation, the nickel(II) center can be oxidized to a nickel(III) species, which also implies the formation of a paramagnetic entity. One-electron oxidations of nickel(II) porphyrins to either the radical cation or the nickel(III) species have been reported before²¹⁻²³, but not in combination with nitronium tetrafluoroborate as the oxidant. As an additional experiment, we also performed the nitration reaction under the standard conditions on **Ni1** to investigate the outcome of the regioselectivity. Interestingly, all selectivity for nitration on the xylylene sidewalls appeared to be lost. ^1H NMR (Supporting Information, Figure S3) and MALDI-TOF (Supporting Information, Figure S4) analysis showed the formation of a mixture of many different nitrated species. This confirms our findings that protonation of the porphyrin ring plays an essential role in the regioselectivity of

the nitration reaction on **H₂1**. From the above experiments we cannot completely exclude that the nitronium ion is first bound in the cavity of **H₂1** before it nitrates the xylylene sidewalls of this compound in a regioselective fashion. What is evident is that the first step of the reaction is the protonation of the porphyrin ring, which protects it from being oxidized or nitrated. These claims are confirmed by the loss of regioselectivity that takes place during nitration after nickel is inserted in the porphyrin ring.

3. Conclusions

We have optimized the synthesis of porphyrin cage compound **H₂1** by reducing the number of steps by two, and alongside increased the yields of the other steps. As such, the overall yield of the bottom part of the cage compound has been increased from 11 to 31%. Moreover, the yield of the final step, in which the bottom part is connected to the porphyrin, could be increased to 58%. We have gained more insight into the possible mechanisms involving the regioselective nitration of cage compound **H₂1**. The high regioselectivity is most probably not caused by the location of the nitronium cation in the cavity of the cage molecule, but controlled by an initial double protonation of the porphyrin ring, which deactivates it for electrophilic aromatic substitution.

4. Experimental

4.1. General Information

Catechol was recrystallized successively from toluene and chloroform and stored in the freezer under an argon atmosphere. Pyrrole was either filtered through a pad of Alumina I just before use or it was distilled under reduced pressure and stored in the freezer under an argon atmosphere. Dichloromethane was distilled from calcium hydride under a nitrogen atmosphere. Other solvents and reagents were obtained from commercial suppliers and used without further purification. Reactions were followed using thin-layer chromatography (TLC) on silica gel-coated plates (Merck 60 F254). Detection was performed with UV light at 254 nm and/or by charring at 150 °C after dipping in a solution of KMnO₄. Column chromatography was performed manually using Acros silica gel, 0.035–0.070 mm, 60A, and Acros aluminium oxide, 0.050–0.200 mm, 60A. NMR spectra were recorded at 298 K on an Agilent Inova 400 spectrometer (400 MHz) equipped with a dual-channel inverse probe, on a Bruker Avance III 500 spectrometer (500 MHz) equipped with a Prodigy BB cryoprobe and on a Bruker Avance III 400 spectrometer (400 MHz) equipped with a BBFO probe. ¹H

NMR chemical shifts (δ) are given in parts per million (ppm) and were referenced to tetramethylsilane (0.00 ppm). Coupling constants are reported as J values in Hertz (Hz). Data for ^1H NMR spectra are reported as follows: chemical shift (multiplicity, coupling constant, integration). Multiplicities are abbreviated as s (singlet), d (doublet), t (triplet), m (multiplet), b (broad). Mass spectra were recorded on a Thermo Finnigan LCQ Advantage Max mass spectrometer (MS), an JEOL AccuTOF CS JMS-T100CS mass spectrometer or on a Bruker Microflex LRF MALDI-TOF system in reflective mode employing dithranol as a matrix.

4.2. Typical synthesis procedures

4.2.1. *1,6:3,4-Bis(2-oxapropylene)tetrahydro-3a,6a-diphenylimidazo[4,5-d]imidazole-2,5(1H,3H)-dione (5)*

TFA (24 mL, 0.31 mol, 1.25 equiv) was added to a solution of urea (31 g, 0.51 mol, 2.05 equiv) and benzil (53 g, 0.25 mol, 1.0 equiv) in toluene (500 mL). The resulting mixture was refluxed for 26 hours in a Dean–Stark apparatus under an argon atmosphere. Upon completion of the reaction, indicated by the disappearance of the yellow color, the mixture was allowed to cool to 20 °C. The resulting precipitate was successively filtered off, washed with ethanol (100 mL) and dried under high vacuum to afford diphenylglycoluril (74 g, 99%) as a white solid. Paraformaldehyde (23 g, 0.78 mol, 5.0 equiv) was added to a suspension of diphenylglycoluril (46 g, 0.16 mol, 1.0 equiv) in DMSO (250 mL). The pH of the reaction mixture was adjusted to 10 by the dropwise addition of aqueous 1M NaOH. The resulting pale yellow solution was stirred at 20 °C for 16 hours. Then, the pH of the reaction mixture was adjusted to 1 by the addition of aqueous 37% HCl. The resulting mixture was refluxed for 2 hours. The suspension was allowed to cool to 20 °C and water (100 mL) was carefully added while stirring. The resulting precipitate was successively filtered off, washed with water (100 mL) and cold ethanol (100 mL), and dried under high vacuum to afford cyclic ether **5** (37 g, 61%) as a white solid. ^1H NMR (400 MHz, CDCl_3) δ 7.20–7.10 (m, 10H), 5.66 (d, $J = 11.2$ Hz, 4H), 4.57 (d, $J = 11.2$ Hz, 4H). Spectral data were in agreement with literature values²⁴.

4.2.2. *1,2-Di-(4-methylbenzene-sulfonyloxy)ethane (6)*

A solution of KOH (33 g, 0.59 mol, 2.6 equiv) in water (800 mL) was purged with argon for 60 minutes. Then, catechol (25 g, 0.23 mol, 1.0 equiv) was added and the reaction mixture was heated to 60 °C. 2-Chloroethanol (50 mL, 0.75 mol, 3.3 equiv) was added dropwise over 15 minutes and the solution was stirred at 60 °C for 99 hours under an argon atmosphere. Additional 2-chloroethanol was added after 24 hours (50 mL, 0.75 mol, 3.3 equiv), 48 hours

(50 mL, 0.75 mol, 3.3 equiv), and 72 hours (25 mL, 0.38 mol, 1.7 equiv). Meanwhile, KOH pellets were added to keep the pH of the reaction mixture between 9 and 11. Upon completion, the mixture was cooled to 20 °C and the product was extracted with DCM (4 × 400 mL). The combined organic extracts were dried over sodium sulfate and the solvent was removed in vacuo. The residue was dissolved in THF (150 mL) at 40 °C and precipitated by the addition of n-heptane (50 mL). The precipitate was successively filtered off, washed with n-pentane (200 mL) and dried under high vacuum to afford the diol intermediate (44 g, 98%) as a white solid. Pyridine (110 mL, 1.3 mol, 6.0 equiv) was added to a 0 °C solution of the diol intermediate (44 g, 0.22 mol, 1.0 equiv) in dry DCM (500 mL). Then, TsCl (130 g, 0.67 mol, 3.0 equiv) was added portion-wise over 15 minutes, the ice bath was removed and the resulting mixture was stirred at 20 °C for 23 hours. The mixture was then diluted with DCM (500 mL). The organic layer was successively washed with water (800 mL), aqueous 6M HCl (600 mL), water (600 mL), and brine (600 mL); then dried over sodium sulfate, after which the solvent was removed in vacuo. The residue was recrystallized from toluene (300 mL) to afford ditosylate **6** (84 g, 78%) as a white solid. ¹H NMR (400 MHz, CDCl₃) δ 7.83–7.78 (m, 4H), 7.36–7.30 (m, 4H), 6.93–6.87 (m, 2H), 6.84–6.78 (m, 2H), 4.35–4.29 (m, 4H), 4.19–4.13 (m, 4H), 2.44 (s, 6H). Spectral data were in agreement with literature values¹⁰.

4.2.3. *Tetratosyl clip (7)*

Method A: Thionyl chloride (7.7 mL, 100 mmol, 20 equiv) was added to a suspension of cyclic ether **5** (1.9 g, 5.0 mmol, 1.0 equiv), ditosylate **6** (6.3 g, 2.5 mmol, 2.5 equiv) and zinc chloride (6.1 g, 45 mmol, 9.0 equiv) in dry DCM (50 mL). The resulting dark blue mixture was stirred at 20 °C for 24 hours under an argon atmosphere. The mixture was diluted with DCM (100 mL) and washed with aqueous 1M HCl (2 × 100 mL) and brine (100 mL). The yellow-orange organic layer was dried over sodium sulfate and the solvent was removed in vacuo. The residue was triturated with acetone (40 mL) and kept at 4 °C for 30 minutes. The precipitate was successively filtered off, washed with acetone (40 mL) and dried under high vacuum to afford clip molecule **7** (3.3 g, 50%) as a white solid. *Method B:* Thionyl chloride (42 mL, 0.58 mol, 15 equiv) was added to a suspension of cyclic ether **5** (14.9 g, 39.5 mmol, 1.0 equiv), ditosylate **6** (43.1 g, 85.1 mmol, 2.1 equiv) and tin(II) trifluoromethanesulfonate (3.36 g, 8.1 mmol, 0.2 equiv) in dry DCM (500 mL). The resulting dark green mixture was stirred at 20 °C for 120 hours under an argon atmosphere. Upon completion, the mixture was washed with water (2 × 500 mL) and brine (500 mL). The yellow-orange organic layer was dried over sodium sulfate and the solvent was removed in vacuo. The residue was triturated

with acetone (400 mL) and kept at 4 °C for 30 minutes. The precipitate was successively filtered off, washed with acetone (200 mL) and dried under high vacuum to afford clip molecule **7** (20.7 g, 39%) as a white solid. ¹H NMR (400 MHz, CDCl₃) δ 7.72–7.66 (m, 8H), 7.21–7.15 (m, 8H), 7.15–7.06 (m, 10H), 6.67 (s, 4H), 4.65 (d, *J* = 15.9 Hz, 4H), 4.21 (t, *J* = 4.7 Hz, 8H), 4.09 (d, *J* = 15.8 Hz, 4H), 3.96 (dt, *J* = 11.5, 4.5 Hz, 4H), 3.91 (dt, *J* = 11.4, 4.8 Hz, 4H), 2.38 (s, 12H). Spectral data were in agreement with literature values¹⁰.

4.2.4. 5,10,15,20-Tetrakis(2-hydroxyphenyl)porphyrin (**8**)

A mixture of 2-methoxybenzaldehyde (14 g, 0.10 mol, 4.0 equiv) and zinc acetate dihydrate (5.5 g, 25 mmol, 1.0 equiv) in propionic acid (500 mL) was heated to reflux. Then, pyrrole (6.9 mL, 0.10 mol, 4.0 equiv) was added dropwise over 10 minutes and refluxing was continued for 2 hours. The resulting black mixture was slowly cooled to 20 °C. The resulting precipitate was successively filtered off, washed with propionic acid (100 mL) and methanol (4 × 50 mL), and dried under high vacuum to afford a dark purple solid. The solid material was dissolved in chloroform (100 mL), DDQ (2.7 g, 13 mmol, 0.5 equiv) was added and the resulting mixture was refluxed for 2 hours. Upon cooling, the mixture was purified by Alumina III column chromatography (eluent CHCl₃). The purified material was dissolved in chloroform (100 mL) and successively washed with aqueous 37% HCl (100 mL), saturated aqueous NaHCO₃ (250 mL); then dried over sodium sulfate, after which the solvent was removed in vacuo. The residue was dissolved in minimal amount of DCM and precipitated by the addition of heptane. Most DCM was removed under reduced pressure and the resulting suspension was centrifuged. The supernatant was removed and the precipitate was washed with pentane and dried under high vacuum to afford H₂TMPP (1.24 g, 7%) as a purple solid. Boron tribromide (3.2 mL, 34 mmol, 20 equiv) was added dropwise over 1 minute to a –25 °C solution of H₂TMPP (1.24 g, 1.7 mmol, 1.0 equiv) in dry DCM (25 mL) under an argon atmosphere. The mixture was slowly warmed to 20 °C and stirred for 16 hours. Upon completion, the mixture was poured onto ice water (300 mL). Then, ethyl acetate (250 mL) was added and the biphasic mixture was stirred vigorously. Solid NaHCO₃ was added carefully until the organic phase turned purple. The organic layer was separated and successively washed with saturated aqueous NaHCO₃ (300 mL), dried over sodium sulfate, after which the solvent was removed in vacuo. The residue was purified by silica gel column chromatography (eluent DCM/MeOH, 19:1, v/v). The purified material was dissolved in minimal amount of DCM and the product precipitated by the addition of heptane. Most DCM was removed under reduced pressure and the resulting suspension was centrifuged. The

supernatant was removed and the precipitate was washed with pentane and dried under high vacuum to afford porphyrin **8** (1.16 g, 99%) as a purple solid. ^1H NMR (400 MHz, CDCl_3) δ 8.91 (s, 8H), 8.00–7.92 (m, 4H), 7.77–7.67 (m, 4H), 7.38–7.28 (m, 8H), 4.92 (bs, 4H), –2.79 (bs, 2H). Spectral data were in agreement with literature values¹¹.

4.2.5. Porphyrin cage compound (**H₂1**)

Potassium carbonate (0.88 g, 6.4 mmol, 11 equiv) was added to a solution of tetratosyl clip **7** (0.78 g, 0.57 mmol, 1.0 equiv) and porphyrin **8** (0.43 g, 0.64 mmol, 1.1 equiv) in acetonitrile (700 mL) and the resulting mixture was refluxed for 10 days. After cooling, the mixture was filtered through a pad of Celite and the residue was washed with chloroform until colorless washings were obtained. The combined filtrate was evaporated to dryness and then purified by Alumina III column chromatography (eluent CHCl_3). The purified material was dissolved in a minimal amount of DCM and precipitated by the addition of n-heptane. Most DCM was removed under reduced pressure and the resulting suspension was centrifuged. The supernatant was removed and the precipitate was washed with n-pentane and dried under high vacuum to afford porphyrin cage compound **H₂1** (0.45 g, 58%) as a purple solid. ^1H NMR (400 MHz, CDCl_3) δ 8.76 (s, 4H), 8.67 (s, 4H), 8.07 (d, $J = 7.3$ Hz, 4H), 7.76 (t, $J = 8.0$ Hz, 4H), 7.37 (t, $J = 7.4$ Hz, 4H), 7.34 (d, $J = 8.4$ Hz, 4H), 6.97–6.91 (m, 6H), 6.83–6.78 (m, 4H), 6.20 (s, 4H), 4.30–4.20 (m, 4H), 4.24 (d, $J = 15.8$ Hz, 4H), 4.09–4.01 (m, 4H), 3.74 (d, $J = 15.8$ Hz, 4H), 3.53–3.43 (m, 4H), 3.37–3.30 (m, 4H), –2.73 (bs, 2H). Spectral data were in agreement with literature values¹⁰. A single crystal of this compound, suitable for X-ray analysis, was grown from a CDCl_3 solution at –60 °C. Crystallographic data have been deposited at the Cambridge Crystallographic Data Centre under number CCDC 1913851.

4.2.6. Nickel(II) porphyrin cage compound (**Ni1**)

A solution of **H₂1** (10 mg, 7.4 μmol , 1.0 equiv) and nickel(II) acetate tetrahydrate (37 mg, 0.15 mmol, 20 equiv) in DMF (2 mL) was refluxed for 20 hours. Upon completion of the reaction (confirmed by MALDI-TOF analysis) and after cooling, the mixture was poured into water (40 mL). The formed precipitate was collected by centrifugation and was successively washed with water (30 mL) and methanol (30 mL), and dried under high vacuum. The residue was purified by silica gel column chromatography (eluent $\text{CHCl}_3/\text{MeCN}$, 9:1, v/v). The purified material was dissolved in a minimal amount of DCM and precipitated by the addition of n-heptane. Most DCM was removed under reduced pressure and the resulting suspension was centrifuged. The supernatant was removed and the precipitate was washed with n-pentane

and dried under high vacuum to afford **Ni1** (8.6 mg, 83%) as a dark red solid. ^1H NMR (500 MHz, CDCl_3) δ 8.69 (s, 4H), 8.56 (s, 4H), 7.96 (dd, $J = 7.3, 1.8$ Hz, 4H), 7.73–7.65 (m, 4H), 7.32 (td, $J = 7.5, 1.1$ Hz, 4H), 7.26 (d, $J = 8.0$ Hz, 4H), 7.01–6.92 (m, 6H), 6.86–6.79 (m, 4H), 6.26 (s, 4H), 4.30 (d, $J = 15.9$ Hz, 4H), 4.24 (ddd, $J = 11.4, 7.8, 4.0$ Hz, 4H), 4.02 (dt, $J = 10.6, 4.2$ Hz, 4H), 3.80 (d, $J = 15.8$ Hz, 4H), 3.52 (dt, $J = 8.6, 4.5$ Hz, 4H), 3.44 (ddd, $J = 10.8, 7.8, 3.9$ Hz, 4H). ^{13}C NMR (126 MHz, CDCl_3) δ 158.44, 157.16, 146.65, 143.67, 143.35, 134.81, 133.44, 131.34, 131.07, 130.58, 129.94, 129.54, 128.56, 128.48, 128.09, 119.78, 115.61, 115.05, 111.72, 84.89, 67.23, 66.50, 44.53. M.p. >300 °C (decomposition). HRMS (ESI) calcd. for $[\text{C}_{84}\text{H}_{62}\text{N}_8\text{NiO}_{10} + \text{Na}]^+$ 1423.38401, found 1423.38381.

Acknowledgements

R.J.M.N. acknowledges support from the European Research Council (ERC Advanced Grant ENCOPOL-74092) and from the Dutch National Science Organization NWO (Gravitation program 024.001.035).

Appendix A. Supplementary data

Supplementary data to this article can be found online at ...

References

1. Trends and Analysis Cisco Company. *White Pap.* June **2017**.
2. J. Gantz, D. Reinzel, in *Proceedings of IDC iView, IDC Anal. Future* **2012**.
3. A. Extance, *Nature* **2016**, *537*, 22–24.
4. P.Y. De Silva, G.U. Ganegoda, *BioMed. Res. Int.* **2016**, *2016*, 14.
5. M. Castillo, *Am. J. Neuroradiol.* **2014**, *35*, 1–2.
6. J.-F. Lutz, *Macromolecules* **2015**, *48*, 4759–4767.
7. G. Cavallo, A. Al Ouahabi, L. Oswald, L. Charles, J.-F. Lutz, *J. Am. Chem. Soc.* **2016**, *138*, 9417–9420.
8. S. Varghese, J.A.A.W. Elemans, A.E. Rowan, R.J.M. Nolte, *Chem. Sci.* **2015**, *6*, 6050–6058.

9. M.G.T.A. Rutten, F.W. Vaandrager, J.A.A.W. Elemans, R.J.M. Nolte, *Nat. Rev. Chem.* **2018**, *2*, 365–381.
10. J.A.A.W. Elemans, M.B. Claase, P.P.M. Aarts, A.E. Rowan, A.P.H.J. Schenning, R.J.M. Nolte, *J. Org. Chem.* **1999**, *64*, 7009–7016.
11. J.A.A.W. Elemans, E.J.A. Bijsterveld, A.E. Rowan, R.J.M. Nolte, *Eur. J. Org. Chem.* **2007**, 751–757.
12. S. Varghese, B. Spierenburg, A. Swartjes, P.B. White, P. Tinnemans, J.A.A.W. Elemans, R.J.M. Nolte, *Org. Lett.* **2018**, *20*, 3719–3722.
13. S. Varghese, B. Spierenburg, J.P.J. Bruekers, A. Swartjes, P.B. White, J.A.A.W. Elemans, R.J.M. Nolte, *Eur. J. Org. Chem.* **2019**, 3525–3533.
14. S. Ostrowski, D. Szerszén, M. Ryszczuk, *Synthesis* **2005**, 819–823.
15. S. Ostrowski, S. Grzyb, *Tetrahedron Lett.* **2012**, *53*, 6355–6357.
16. F. Ji, L. Zhu, X. Ma, Q. Wang, H. Tian, *Tetrahedron Lett.* **2009**, *50*, 597–600.
17. W.J. Kruper, T.A. Chamberlin, M. Kochanny, *J. Org. Chem.* **1989**, *54*, 2753–2756.
18. M. M. Catalano, M. J. Crossley, M. M. Harding, L. G. King, *J. Chem. Soc., Chem. Commun.* **1984**, 1535–1536.
19. J. Baldwin, M. J. Crossley, J. DeBernardis, *Tetrahedron* **1982**, *38*, 685–692.
20. P. Hidalgo Ramos, R. Coumans, A. B. C. Deutman, R. de Gelder, J. M. M. Smits, J. A. A. W. Elemans, R. J. M. Nolte, A. E. Rowan, *J. Am. Chem. Soc.*, **2007**, *129*, 5699–5702.
21. D. Chang, T. Malinski, A. Ulman, K.M. Kadish, *Inorg. Chem.* **1984**, *23*, 817–824.
22. G.S. Nahor, P. Neta, P. Hambright, L.R. Robinson, *J. Phys. Chem.* **1991**, *95*, 4415–4418.
23. J. Seth, V. Palaniappan, D.F. Bocian, *Inorg. Chem.* **1995**, *34*, 2201–2206.
24. F.G.M. Niele, R.J.M. Nolte, *J. Am. Chem. Soc.* **1988**, *110*, 172–177.

Highlights:

- Porphyrin cage compounds based on diphenylglycoluril can be synthesized in 8 steps in batches up to 450 mg
- Porphyrin cage compounds can be selectively nitrated at their cavity side-walls
- Protonation of the porphyrin plane causes nitration by electrophilic nitronium ions to be directed to the cavity side-walls